FROST RESISTANCE OF STEEL FIBRE HIGH STRENGTH CONCRETE

Sirje Vares, Research Scientist

Technical Research Centre of Finland
Building Technology
Concrete and Minerals Technology

VTT/RTE
PL 1805
02044 VTT
Finland

ABSTRACT

The main objective of this work was to investigate the influence of Dramix steel fibres on the microstructure of steel fibre reinforced concrete (SFRC) and the influence of the microstructure on frost resistance. This work is part of the investigation "Fibre-reinforced high-strength concrete" Vares & Häkkinen /15/. The frost resistance of SFRC with 2% and 4% steel fibres was determined after subjecting the concretes to 100 and 200 freeze-thaw cycles, by comparing changes of strength, toughness and micro-structure with those of specimens stored in water. No serious damages to the SFRC microstructure was observed after 200 freeze-thaw cycles.

Key words: Steel fibre reinforced concrete (SFRC), frost resistance, compressive and flexural strength, toughness, microstructure.

1 INTRODUCTION

The principle of hydraulic pressure is one of the most applied theories of frost resistance. Probably the main reason for its common use is its perspicuous character and easiness. The presenter of this theory, Powers, stated that not only the hydraulic pressure, but also diffusion phenomena affect the degree of frost damage /10/, /12/. The expansion of water during freezing is roughly 9%, causing hydraulic pressure in the pores of concrete. When water freezes in a capillary pore the expanding ice forces water through the hydrated cement paste towards the air pore. The shorter the distance to the nearest air pore, the easier is the movement of water and the lesser the development of hydraulic pressure through the concrete. The pressure is greater the greater the distance to the closest air pore or surface of the concrete /11/. Most frost resistance theories are based on freezing of water and its moisture movement in concrete.

Hydraulic pressure increases the formation and growth of cracks and coarsening of pore structure. Crystallization pressure of ice /4/, osmotic pressure /17/ and formation of ice lenses /5/ should cause cracking to develop mostly parallel to the concrete surface.

Thermal incompatibility /16/, /6/ causes cracks to develop in concrete especially near the aggregate surfaces. This degradation mechanism increases cracking but does not change pore size distribution.

The theory of frost resistance determination based on the critical degree of saturation was proposed by Fagerlund /13/. The degree of saturation is the volume of pores filled with water divided by the total pore volume. Fagerlund has shown that a porous material is damaged upon freezing only if its water content is higher than the given critical degree of saturation. More detailed theories of concrete frost resistance and frost effects on the microstructure of high strength concrete have been studied by Kukko /8/.

According to ACI, the ASTM C 666 Standard Test Method for "Resistance of Concrete to Rapid Freezing and Thawing" /2/ is applicable to fibre reinforced concrete. The relative dynamic modulus of elasticity method, described by ASTM C 666, is also appropriate for fibre reinforced concrete.

In this work, using freeze-thaw tests capillary immersion measurement was performed using the method developed by Fagerlund, for estimation of water suction properties, capillary porosity and frost resistance. The freeze-thaw cycling was arranged according to Finnish Standard SFS 5447. The frost damage of concrete after freeze-thaw tests /14/ was studied in terms of mean strength and toughness.

2 MATERIALS AND PROPORTIONS

White Portland cement and silica fume were used as binding materials for concrete and SFRC. Cement, produced by the Aalborg Portland Cement Factory, was used, as it lowers the water demand of the concrete mix compared with that of Portland cement produced in Finland.

30 mm Dramix steel fibres were used, with density 7800 kg/m^3, modulus of elasticity 210 GPa and tensile strength 1000 MPa.

The water reducing agent (superplasticizer), Super-Parmix (modified naphthalene-formaldehyde polycondensate) was used.

The concrete proportions are given in the Table 1.

Table 1. Concrete proportions.

Concrete	a/b	w/b	Fibre vol.	Binder %		Aggregate %		Super-plasticizer *
			%	Cement	Silica	Fine sand	Coarser sand	%
A1	2	0.32	0	90	10	milled quartz 51	0.1 - 3 mm 49	6
A2	2	0.34	2	90	10	milled quartz 51	0.1 - 3 mm 49	6
A3	2	0.36	4	90	10	milled quartz 51	0.1 - 3 mm 49	6
B2	4	0.36	2	90	10	-	0.1 - 3 mm 100	3
B3	4	0.4	4	90	10	-	0.1 - 3 mm 100	3
C3	4	0.48	4	80	20	-	0.1 - 3 mm 100	3

a/b - aggregate-binder ratio,
w/b - water-binder ratio,
* - % from the weight of binder

3 TEST METHODS

3.1 Frost resistance

Steel fibre reinforced concrete (SFRC) types B2 and B3 with 2% and 4% of steel fibre respectively was subjected to the freeze-thaw cycling according to Finnish Standard SFS 5447 /14/. Specimens measuring 40 x 40 x 160 mm^3 were prepared and their strength and toughness parameters determined after freeze-thaw cycling. The specimens were frozen and thawed in the freezing chamber. The temperature changes during one freeze-thaw cycle are presented in Figure 1.

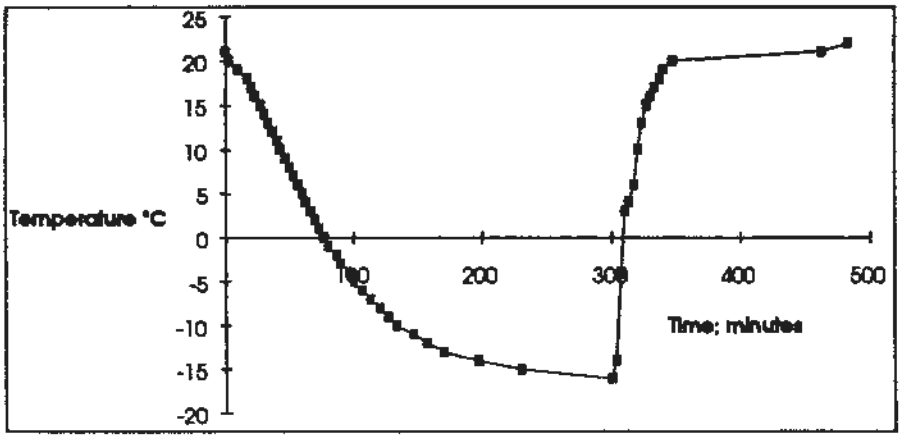

Figure 1. Temperature changes during the one freeze-thaw cycle.

The specimens were subjected to 100 and 200 freeze-thaw cycles. The reference specimens were cured in water at 20°C. The frost durability of SFRC was assessed from strength and toughness losses. The influence of freeze-thaw cycles on cracking of the structure was determined with using microscopic examination.

3.2 Compressive and flexural strength

The study focused on the determination of compressive strength (f_c), flexural strength (f_{ft}) and toughness (I_5, I_{10}, I_{20}, T_b) of SFRC reference specimens and specimens after freeze-thaw cycling. The specimens were tested for flexure with loading on the 120 mm span. The testing machine produces a constant rate of increase in specimen deflection. The deflection, increased by a velocity of 0.5 mm/min, was determined by an electronic transducer placed at the specimen mid-span. During the tests, load force (F) and load point deflection (d) curves were recorded up to 3 mm deflection. The typical curves obtained are shown in Figure 2, where F_u - ultimate (maximum) force; F_{fc} - force at the point of first crack; d_u - deflection at the point of ultimate force; d_{fc} - deflection at the point of first crack; T_b - fracture energy /7/.

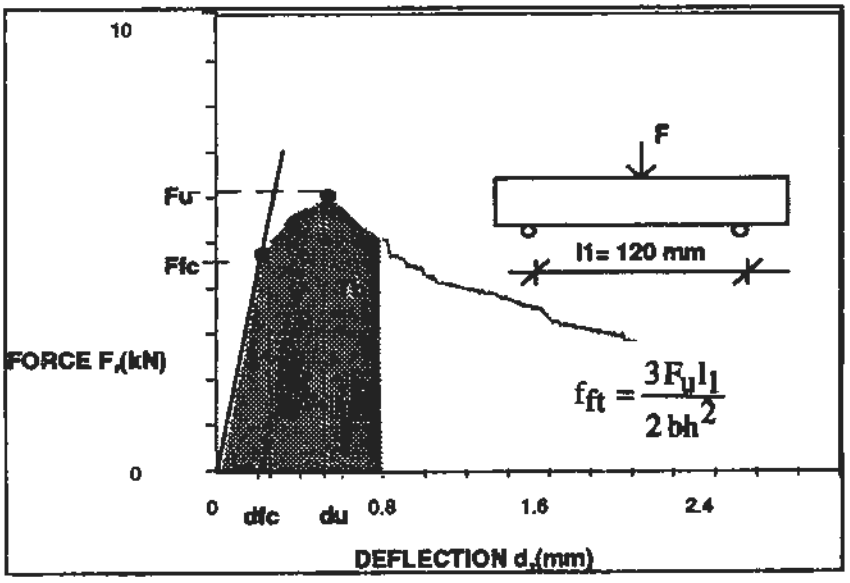

Figure 2. Typical load-deflection curve for SFRC obtained in the flexure test.

The remaining halves of the specimens from the flexural test were used for the compressive test. The compressive area was 40 x 40 mm^2.

3.2.1 Calculation schemes

In this paper the toughness of SFRC is estimated according to ASTM Standard C 1018-92 /3/ and the Japanese Concrete Institute Standards JCI SF4 /7/.

According to ASTM C 1018-92, the material toughness is characterised by means of toughness indices I_5, I_{10} and I_{20}. The toughness indices I_5, I_{10} and I_{20} are the ratios between the areas under the load-deflection curve up to 3.0, 5.5 and 10.5 times the first crack point and that under the deflection curve up to the first crack point.

$$I_5 = W(3d_{fc}) / W(d_{fc}); \quad (1)$$

$$I_{10} = W(5,5d_{fc}) / W(d_{fc}); \quad (2)$$

$$I_{20} = W(10,5d_{fc}) / W(d_{fc}); \quad (3)$$

The load-deflection (F - d) curve in figure 2 characterises the material resistance to fracture in terms of energy. In equations 1 - 3, d_{fc} is the deflection at the point where the first estimated crack occurred (Figure 2); $W(d_{fc})$ is the work of external forces up to the first crack deflection, and $W(3\ d_{fc})$, $W(5.5\ d_{fc})$ and $W(10.5\ d_{fc})$ are the work of external forces up to the specified deflection.

Material behaviour tougher than "elastic ideal plastic" material corresponds to the indices I_5, I_{10} and I_{20} greater than 5, 10 and 20. The method of calculation of toughness indices is readily adaptable to specimens of different shapes and sizes. The shape of the load-deflection curve can be quantified in such a way that the first-crack area is used as the denominator in the toughness index calculation.

On the curve the material elastic stage was approximated by the straight line, and the first crack load (F_{fc}) was estimated at the point where curve F - d deflects from the straight line.

The stiffness K is a mechanical parameter that characterises the deformation behaviour of a fibre composite at the elastic stage:

$$K = \frac{F_{fc}}{d_{fc}} \qquad (4)$$

The Japanese Concrete Institute (JCI) defines toughness (T_b) in absolute terms as the energy required to deflect an SFRC beam to a mid-point deflection of l_1/150th of its span. In our test the span of flexure was 120 mm, and the energy requirement of the material (W) was at point d, where the deflection was 0.8 mm.

3.3 Capillary water absorption

The capillary water absorption test was arranged according to the RILEM Committee 4 CDC recommendation /13/. The capillary water suction test was performed on concrete sections (100 x 100 x 25 mm^3) taken from specimens measuring 100 x 100 x 100 mm^3 to determine the SFRC concrete porosity parameters. The samples were dried at +50°C and placed on a grating to absorb water from below by capillary absorption. The RH of the test room was >95%. The weight of the specimens was measured intermittently for about 3 weeks. Subsequently the specimens were completely saturated at a water pressure of 15 MPa to determine the total amount of pores. Finally the samples were dried at 105°C. The Degree of water saturation is defined by

$$S = V_w/V_p; \qquad (5)$$

where V_w is the total water volume evaporable at +105°C and
V_p is the total open pore volume.

The water saturation rate for different SFRC is expressed as a function of time (square-root scale). The intersection of the curves obtained gives the "nick-point absorption". Before the "nick-point", gel and capillary pore absorption take place, and beyond it is air pore absorption. SFRC porosity parameters were presented as follows: total porosity, air porosity, "gel porosity", capillary porosity and their ratios from total porosity in %, capillary index (k), material water

resistance coefficient (w) and material density. The water resistance and capillary index were calculated as follows:

$$w = 3600\, t_{np} / (0{,}5\, h)^2 \quad (6)$$

$$k = P_{cap}\left(1000\sqrt{w}\right) \quad (7)$$

where
- w is water resistance
- t_{np} nick-point time
- h height of the specimen
- k capillary index
- P_{cap} volume of pores filled with water in time t.

3.4 Microscopic examination

Thin sections measuring roughly 15 x 30 x 40 mm^3 were cut from the samples using a thin blade diamond saw and impregnated in a vacuum with epoxy resin containing fluorescent dye. The pieces were glued onto glass plates and thinned to a final thickness of 25 µm by sawing and grinding. The sections were finished by glueing a thin glass cover over the top. Thin sections were prepared according to the NT BUILD 361 method - Concrete, hardened: water-cement ratio /9/.

Porosity and microcracking were observed visually under a polarising and fluorescent microscope. Polarising light microscopy enables pores larger than 5 - 10 µm to be visualised. Air pores with diameter <0.5 mm were assumed to be protective pores and those measuring >0.5 mm to be partly due to inadequate compaction. Cracking was assessed on a cracking index of 0 to 3, where 0 represents no cracking and 3 is strongly cracked concrete. Cracking perpendicular to the aggregate particle or fibre surface is termed shrinkage cracking and that parallel to the surface bond cracking.

Air pores measuring >500 µm and <500 µm were counted by the modified point-count method based on ASTM Standard C 457-90 /1/. Thin sections of different SFRC were examined microscopically along a series of regularly spaced traverse lines. A total of 3000 points per section were counted with a Swift point counter.

4 TEST RESULT

4.1 Compressive- and flexural strength and toughness after freeze-thaw test

The frost resistance of SFRC was evaluated after 100 or 200 freeze-thaw cycles from material strength and toughness losses. Prior to testing the reference specimens were stored in water at 20°C. SFRC compressive strength (f_c), flexural strength (f_{ft}) and toughness parameters (T_b, I_5, I_{10}, I_{20}, K) after freeze-thaw cycling and after storing in water (reference specimens) are presented in Table 2. Load-deflection curves of SFRC (types B2 and B3) in the flexure test after 100 and 200 freeze-thaw cycles and after storing in water are presented in Figures 3 - 4. FRC compressive and flexural strengths after 100 or 200 freeze-thaw cycles are presented in Figure 5.

Table 2. Strength and toughness properties of SFRC type B2 and B3 stored in water and these parameters after SFRC subjected to freeze-thaw cycling.

SFRC	Strength and toughness	7 days in water	40 days in water	74 days in water	100 freeze-thaw cycles	200 freeze-thaw cycles	Ratio
		(1)	(2)	(3)	(4)	(5)	(5)/(2)
B2	f_c (MPa)	86	107	111	101	103	0.96
	f_{ft} (MPa)	13	18	19	14	15	0.83
	T_b (Nm)	2.9	4	4.6	3.2	3.4	0.85
	I_5	5.5	6	5.1	5.8	5.2	0.87
	I_{10}	11	12	10	12	9.6	0.8
	I_{20}	20	21	18	20	17	0.81
	K	34	33	40	37	36	1.09
B3	f_c (MPa)	76	99	105	92	104	1.05
	f_{ft} (MPa)	18	16	24	15	26	1.63
	T_b (Nm)	4.2	3.8	5.6	3.5	5.9	1.55
	I_5	6.1	5.8	5.8	5.5	5.5	0.95
	I_{10}	13	12	12	12	11	0.92
	I_{20}	26	23	22	21	19	0.83
	K	36	32	34	38	36	1.13

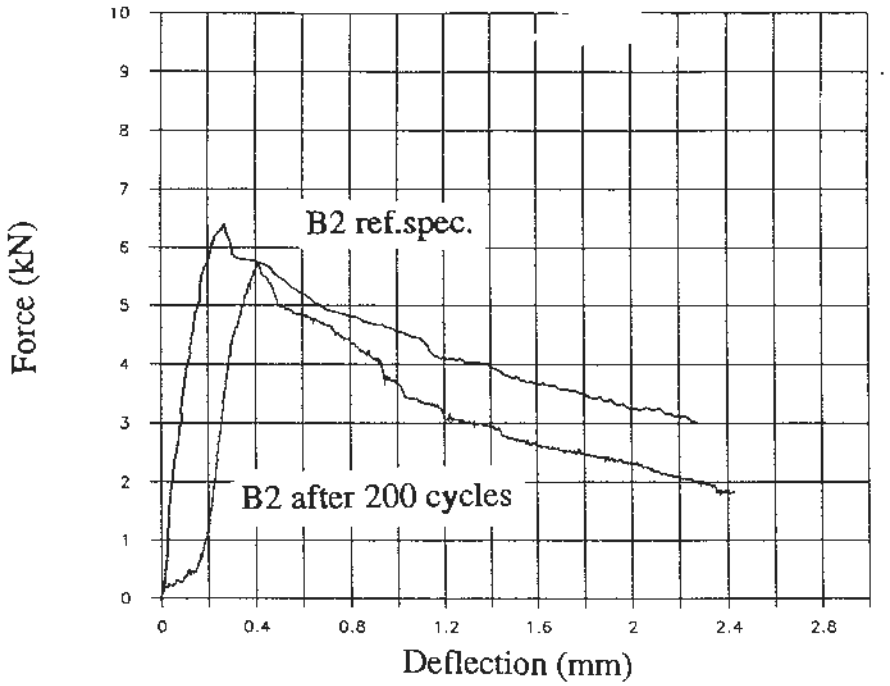

Figure 3. Load-deflection curve for SFRC type B2 after 200 freeze-thaw cycles and for reference specimens after 40d storage in water.

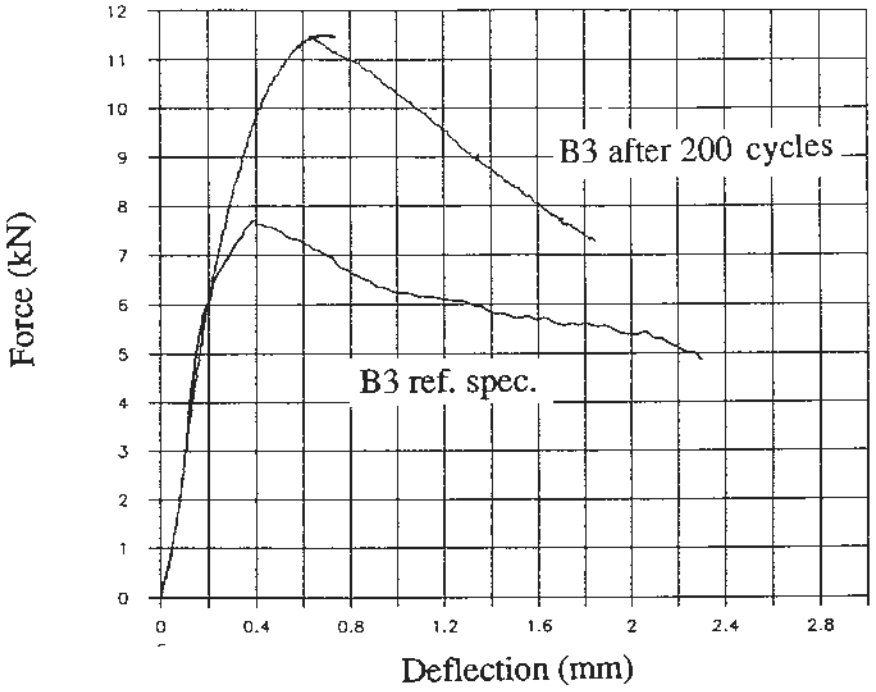

Figure 4. Load-deflection curve for SFRC type B3 after 200 freeze-thaw cycle and for reference specimens after 40d storage in water.

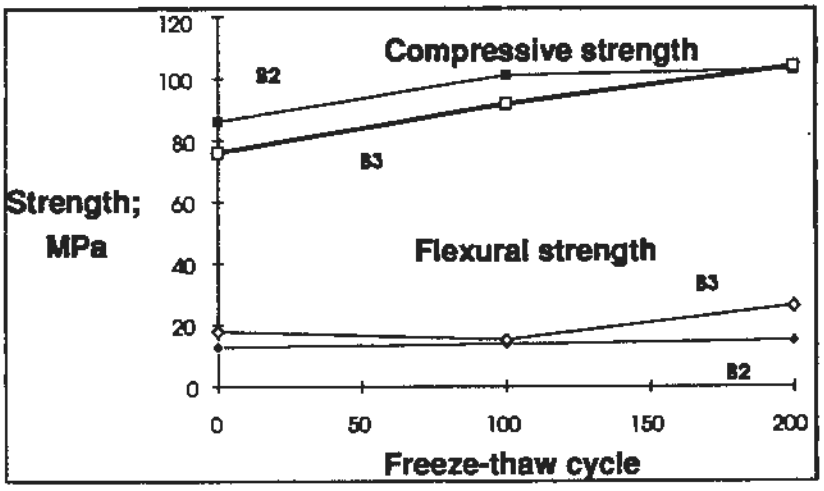

Figure 5. SFRC strength after 100 or 200 freeze-thaw cycles.

4.2 Microstructure

Table 3 shows the cracking of concrete thin sections after frost exposure estimated visually with an optical microscope. Table 4 shows the SFRC air porosity distribution calculated from thin sections.

Table 3. Thin section optical analysis for reference SFRC and for SFRC subjected to freeze-thaw cycling. Notation : S - shrinkage type cracking; B - bond type cracking.

No. of cycles	Age day	Concrete B2 (Dramix 2%)		Concrete B3 (Dramix 4%)	
		Cracking index	Cracking description	Cracking index	Cracking description
0	7	0.5	S + B.	0	-
0	40	0.5	B	0.5	B
100	40	0.5	S + B	0.5	B
0	74	1.5	S + B	1	S + B
200	74	1	S + B	1	S + B

Table 4. SFRC air porosity distribution from thin sections (results by the modified point-count method - ASTM C 457 - 90).

SFRC	Air pores <500 µm, %	Air pores >500 µm, %	Fibre content in thin section, %	Pore (<500 m) distance; mm	Mortar %
A1	3.1	0.6	0	0.46	58
A3	4.7	1.0	5	0.29	48
B3	4.7	4.9	6	0.24	26
C3	3.9	1.5	6	0.28	31

4.3 Capillary water permeability and pore size of tested concretes

The air, capillary and "gel" porosity of SFRC were determined (Table 5) using the capillary water saturation method.

Table 5. Porosity parameters. Notation: k - capillary index and w - water resistance.

SFRC		A1	A2	A3	B3	C3
Total porosity	l/m^3	123	164	204	185	190
Air pore	l/m^3	25	51	98	90	74
Capillary pore	l/m^3	15	23	20	39	51
Gel pore	l/m^3	84	90	86	56	65
Air pore ratio		0.20	0.31	0.48	0.48	0.39
Capillary pore ratio		0.12	0.14	0.10	0.21	0.27
Gel pore ratio		0.68	0.55	0.42	0.30	0.34
k	$kg/m^2\sqrt{s}$	0.002	0.004	0.004	0.007	0.008
w	s/mm^2	49	40	32	35	38

The gel pores formed during the cement hydrating process are assumed to have a mean magnitude of 0.0015 to 0.0020 µm, the capillary pores a mean magnitude of 1 µm and air pores a mean magnitude of 0.01 to 0.5 mm.

5 DISCUSSION

The concrete pore structure was studied as a possible factor influencing to frost resistance of fibre reinforced concrete. On the basis of the capillary suction method the following conclusions can be drawn:

- Concrete reinforced with fibres had increased air porosity (Table 5). In Figure 6 the rate of air porosity correspond to the value of S_{np} (S nick-point) up to the two intersection lines.
- The matrix composition and fibre content influenced the air porosity and density of concrete. Depending on the fine sand content, and therefore tightness, concretes dried at +105°C lost different amount of water, considered to be in "gel" pores. Figure 7 shows the "gel" porosity rate, which is the starting value of the first curve.
- A higher fibre content leads to higher air porosity of the concrete (Table 5 and Figure 8).

The additional air porosity could be due to the mixing technique and poor compaction which is the result of the poor fibre-matrix interface. High fibre volumes make fresh concrete very sticky, so that air brought in during mixing is arrested and vibration does not remove it efficiently.

Despite their higher porosity, the SFRCs had the low capillary water permeability, with capillary index < 0.01 kg/m$^2\sqrt{s}$ (Table 5).

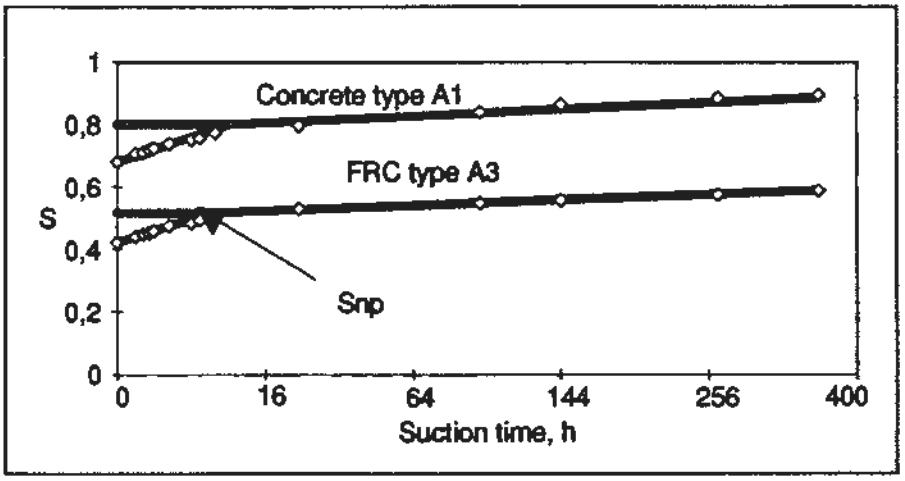

Figure 6. Capillary water suction of SFRC (type A3) and concrete without fibres (type A1).

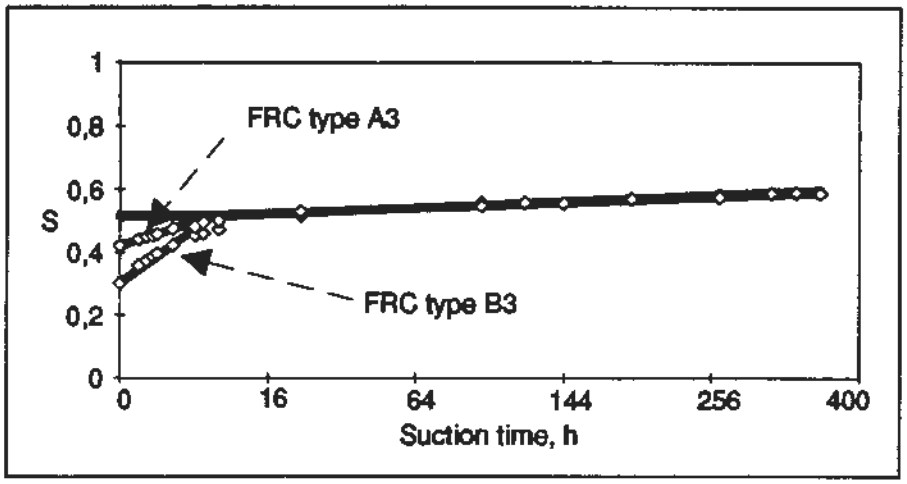

Figure 7. Capillary water suction of SFRC with higher sand content (type A3) and SFRC with smaller sand content (type B3).

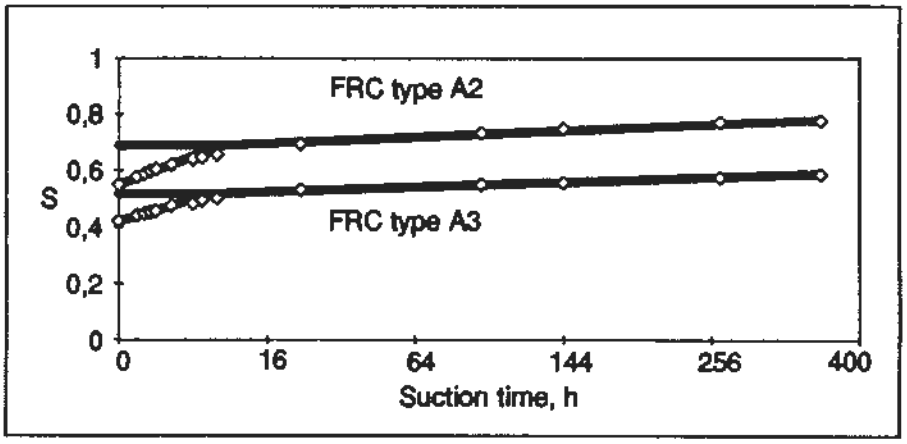

Figure 8. Capillary water suction of SFRC with higher fibre volume content - 4 vol.% (type A3) and SFRC with smaller fibre content - 2 vol.% (type A2).

The air porosity distribution was determined from thin-sections by the point-count method (ASTM C 457 - 90). The compaction pores were assumed to be higher than 500 µm and the protective air pores to be smaller than 500 µm. Concrete turns tighter and less porous (compaction pores) with fine sand fractions. The increase of amount of fine sand in SFRC decreases the rate of compaction pores in concrete (Table 4; 1).

The amount of compaction pores in SFRC decreased when silica fume content was increased (Table 4, 1).The silica phenomenon is based on its fineness and pozzolanic reaction with $Ca(OH)_2$.

The thin section analysis shows that investigated SFRC-s had more air pores with diameter d < 0,5 mm than FRC. The distance between these air pores was about 0,24 - 0,3 mm (Table 4). This improves the frost resistance of concrete. Very likely the fibres split the air pores into smaller units during mixing and compaction so the air pore distance becomes smaller and the frost resistance becomes better.

The frost resistance of SFRC was analysed by comparing the material mechanical parameters after 200 freeze-thaw cycles with the results of the reference specimens cured for 40 days in water. The period of 40 days corresponds to the time when the specimens during cycling were at the temperature of above 0°C. According to the results the freeze-thaw cycling decreased the strength and toughness of the SFRC with 2 % fibre: the compressive strength decreased by 4%, flexural strength by 17% and toughness indeces by 13 - 20%. For concrete with 4% fibres the strength parameters increased, but the toughness indeces decreased by 5 - 17%, which were not so significant as for concrete with 2% of fibres (Table 2). SFRC with such a small water-binder ratio invariably contained unhydrated cement particles, which upon with water increase the hydration of concrete. Possibly freezing and thawing caused some microcraking, which was not observed in the thin-sections. This slight destruction of the matrix was nonetheless sufficient for unhydrated cement particles along the microcracks to make contact with additional water and to react, producing calcium hydroxide which strengthens the fibre-matrix interface. This increased hydration raised the flexural strength of SFRC with a 4% fibre content after 200 freeze-thaw cycles over that of the reference concrete stored in water. However, with a fibre content of 2% no such effect was observed.

Thin-section analyse for concrete B2 and B3 showed that the cracking of material structure after 200 freeze-thaw cycles was no grater than with the reference specimens. The amount of bond type cracking was a little grater than shrinkage type cracking. The bond type cracking indicating poor fibre-matrix contact influences the material strength and toughness (Table 3).

The absolute toughness value T_b calculated by the JCI method is more dependent on flexural strength than the ASTM indices. After 200 freeze-thaw cycles the absolute toughness value for concrete with 2% fibres was decreased by 15%, but for concrete with a higher amount of fibres it increased by 55% compared with the reference specimens stored in water.

The SFRC stiffness K increased by 9 - 13%, which shows that freeze-thaw cycles did not decrease the material elastic resistance. It means that freeze-thaw cycling had no effect on the strengthening process of the material, especially with the concrete B3.

When the percentage of fibre volume in SFRC is small (1 -2%), slight damage to fibre-matrix interface during freezing and thawing makes the concrete more sensitive to mechanical influences.

6 CONCLUSIONS

Steel fibres modify the microstructure of concrete by increasing porosity. A higher fibre content leads to higher air porosity of the concrete. A high fibre volume makes fresh concrete very sticky so that air brought in during mixing is arrested and vibration does not remove it effectively. Additional fine components reduce the number of compaction pores and make the concrete tighter.

Despite their higher porosity, the SFRC has a low capillary water permeability.

The optical investigation shows that the greater part of the thin sections had bond type cracking, indicating poor fibre-matrix contact.

In SFRC there were found appropriate spacing and air pore sizes (< 0.5 mm) advantageous for the freeze-thaw durability.

According to the results the freezing and thawing of the SFRC with 4% fibres had increased flexural strength and decreased toughness. Possibly the increased hydration raised the flexural strength of SFRC with a 4% fibre content after 200 freeze-thaw cycles over that of the reference concrete stored in water. However, with a fibre content of 2% no such effect was observed.

The absolute toughness values T_b calculated by the JCI method are more sensitive to the flexural strength than the ASTM indices. When the percentage of fibre volume in concrete is small (1 - 2%), slight damage to fibre-matrix interface during freezing and thawing makes the concrete more subject to mechanical influences. For example, the absolute toughness value reduced as much as by 15% in the case of SFRC with 2% steel fibres, but increased by 55% in the case of SFRC with 4% steel fibres.

It was observed that concrete with 2 vol.% and 4 vol.% of steel fibres withstood to the expanding ice during freezing and no serious damages to the SFRC structure was observed after 200 freeze-thaw cycles. Thin-section analysis showed that the cracking after 200 freeze-thaw cycles, in terms of cracking index, was no grater in SFRC investigated than compared with those stored in water.

7 REFERENCES

/1/ ASTM C 457-90. 1990. Standard test method for microscopical determination of parameters of the air-void system in hardened concrete. Philadelphia, PA: American Society for Testing and Materials. 13 p.

/2/ ASTM C 666. 1990. Standard test method for resistance of concrete to rapid freezing and thawing. Philadelphia, PA: American Society for Testing and Materials.

/3/ ASTM C 1018-92. 1992. Standard test method for flexural toughness and first-crack strength of fibre-reinforced concrete (using beam with third-point loading). Philadelphia, PA: American Society for Testing and Materials. 7 p.

/4/ Collins, A. R. 1944. The destruction of concrete by frost. Journal of the Institution of Civil Engineers. 23, 1, pp. 29 - 41.

/5/ Everett, D. H. 1961. The thermodynamics of frost damage to porous solids. Transactions of the Farady Society. 57, pp. 1541 - 1551.

/6/ Huovinen, S. 1990. Abrasion of concrete by ice in artic sea structures. Espoo, Technical Research Centre of Finland, Publications 62. 110 p. + app. 31 p.

/7/ JCI SF4. Japan Concrete Institute. 1983. Method of test for flexural strength and flexural toughness of fibre reinforced concrete. In: JCI Standards for test methods of fiber reinforced concrete. pp. 45 - 51.

/8/ Kukko, H. 1992. Frost effects on the microstructure of high strength concrete, and methods for their analysis. Technical Research Centre of Finland. Publications 126. 133 p + app. 29 p.

/9/ NORDTEST 1991. NT BUILD 361. Concrete, hardened: water-cement ratio. Espoo: NORDTEST. 4 p.

/10/ Powers, T. C. 1965. The mechanism of frost action in concrete. Collage Park, Md. Stanton Walker Lecture Series on Material Science, Lecture 3. 35 p.

/11/ Powers, T. C. & Helmuth, R. A. 1953. Theory of volume changes in hardened Portland cement paste during freezing. Proceedings, Hghway Research Board 32, 5, pp 285 - 297.

/12/ Powers, T. C. 1975. Freezing effects in concrete. In: Durability of concrete. Detroit; MI; American Concrete Institute, Publication SP - 47. pp. 1 - 11.

/13/ RILEM Committee 4 CDC. 1977. Tentative recommendation. The critical degree of saturation method of assessing the freeze/thaw resistance of concrete. Materials and structures, Vol.10, No. 58, pp. 217 - 229.

/14/ SFS 5447. 1988. Concrete. Durability. Freeze - thaw resistance. Helsinki: Finnish Standards Association. 2 p.

/15/ Vares, S. & Häkkinen, T. 1993. Fibre-reinforced high-strength concrete. Espoo. Technical Research Centre of Finland, Publications 160. 73 p. + app. 13 p.

/16/ Venecanin, S. D. 1983. Stresses in concrete due to the thermal incompatibility of its components. Int. Coll. Material Science and Restauration. Essingen, Germany. pp. 93 - 98.

/17/ Verbeck, G. J. & Klieger, P. 1957. Studies of salt scaling of concrete. Washington. Highway research board, Bulletin 150. 13 p.